

# Compression of femtosecond ytterbium fibre laser pulses using nonlinear processes in silica fibre

N.V. Didenko, A.V. Konyashchenko, L.L. Losev, A.V. Tausenev, S.Yu. Tenyakov

**Abstract.** The temporal compression of 100-fs nanojoule laser pulses using nonlinear processes in silica fibre has been studied by numerical simulation and experimentally. The simulation results demonstrate that, in the case of spectral broadening in a normal dispersion fibre, followed by the temporal compression of the pulse in a compressor with a negative second-order dispersion, up to 90% of the compressed pulse energy can be concentrated in the main peak, whose duration is a factor of 8 shorter than the initial laser pulse duration. In our experiments, 100-fs ytterbium fibre laser pulses have been compressed to pulses with an  $\sim 13$ -fs main peak accounting for 87% of the compressed pulse energy. At an average ytterbium laser output power of 4.2 W, the average power at the compressor output has been 3.1 W.

**Keywords:** femtosecond pulses, silica fibre, temporal compression, self-phase modulation.

## 1. Introduction

Diode-pumped femtosecond lasers based on ytterbium-doped fibre and crystals are currently the most efficient and widely used laser systems. In pulsed mode, they can generate pulses with durations of  $\sim 100$  fs at an average output power above 100 W [1]. The generation of shorter pulses directly in a laser system is impeded by the insufficient gain linewidth of the active medium (except for lasers in which operation modes are possible with broadening of their emission spectrum owing to nonlinear processes directly in their active medium, e.g. in fibres, and with the generation of pulses whose spectrum is broader than the gain band [2]). Because of this, pulses of  $\sim 10$  fs duration are produced using external temporal laser pulse compressors. In most cases, the operation of temporal compressors is based on nonlinear spectral broadening of a pulse during the self-phase modulation process (frequency chirping) as the pulse propagates in a medium with normal (positive) dispersion, followed by pulse compression in a optical component.

Pulses with energies from 1  $\mu$ J to 10 mJ can be compressed using gas-filled hollow fibres (capillaries [3, 4] or hollow-core photonic crystal fibres [5]). In the case of lower pulse energies,

solid-core photonic crystal fibres are used [6, 7]. The energy efficiency of such compressors exceeds 50% and their pulse compression factor (the ratio of the initial laser pulse duration to the compressed pulse duration) is  $\sim 10$ . An inherent drawback of gas-filled fibre compressors that rely on a nonlinear self-phase modulation effect is the relatively low pulse contrast. The temporal compression of a spectrally broadened pulse by a negative-dispersion optical component produces a low-intensity pedestal whose duration approaches the initial laser pulse duration. The reason for the relatively low pulse contrast is that, in the case of nonlinear self-phase modulation, the frequency chirp of the pulse is nonmonotonic and changes sign during the pulse. Because of this, negative-dispersion optical components (diffraction gratings, prisms and chirped mirrors) are typically used to compensate for only a monotonically varying positive chirp that arises in the middle of a pulse. The wings of a negatively frequency-chirped pulse remain uncompressed and form a low-intensity pedestal, which may account for up to 40% of the pulse energy (see below). To improve pulse contrast, use is made of additional nonlinear converters based on harmonic generation, spectral filtering [8], polarisation ellipse rotation [9], etc.

Compared to compression in gases, laser pulse compression in solid-core fibres has a number of distinctive features due to the effect of material dispersion on the nonlinear pulse self-action process. The spectral broadening process occurs in the dispersive self-phase modulation regime [10–12], which opens up the possibility of obtaining a monotonic, nearly linear frequency chirp essentially throughout the laser pulse. At the same time, there are nonlinear effects related to chirped laser pulse steepening [13], which distort a linear frequency chirp and reduce the compressed pulse contrast. In such a case, to obtain high-quality, high-contrast pulses it is necessary to find the range of parameters (diameter and length) of a solid-core fibre that minimise undesirable nonlinear effects.

Previous studies of nanojoule pulse compression in fibre [6, 7, 10–12] were aimed primarily at maximising the spectral bandwidth of chirped pulses and, accordingly, minimising the compressed pulse duration. The contrast of such pulses has not received sufficient attention. In this work, we studied the compression of femtosecond nanojoule ytterbium fibre laser pulses in silica fibre with the aim of obtaining high-contrast pulses of  $\sim 10$  fs duration.

## 2. Numerical simulation

Prior to experiments, we performed numerical calculations of the nonlinear pulse spectral broadening process in silica fibre and subsequent temporal compression. The nonlinear Schrödinger equation was solved numerically with allowance

N.V. Didenko, A.V. Konyashchenko, L.L. Losev, A.V. Tausenev  
P.N. Lebedev Physical Institute, Russian Academy of Sciences,  
Leninsky prosp. 53, 119991 Moscow, Russia; e-mail: lllosev@mail.ru;  
S.Yu. Tenyakov Avesta Ltd., Fizicheskaya ul. 11, Troitsk, 142190  
Moscow, Russia

Received 6 March 2018; revision received 3 April 2018  
*Kvantovaya Elektronika* 48 (5) 476–480 (2018)  
Translated by O.M. Tsarev

for the dispersion in the medium [14]. The calculations were made for a  $\text{sech}^2$  laser pulse of 100 fs duration (full width at half maximum). The laser pulse energy was 15 nJ and the centre wavelength was 1050 nm. We simulated the spectral broadening of the pulse during propagation in a single-mode silica fibre with a mode field diameter of 4  $\mu\text{m}$ . The calculation results are presented in Fig. 1.

To assess the effect of the dispersion in the nonlinear medium, we performed calculations for zero dispersion in the fibre, without changing laser pulse parameters (Fig. 1, column A). Under these conditions, the pulse shape at the output of the active medium is the same as that at its input. The spectrum of the pulse has a multi-peaked structure (with an almost 100% modulation depth), similar to what is observed in experiments with gaseous active media [15]. It is seen from the time dependence of the instantaneous pulse frequency that the sign of the frequency chirp changes twice during the pulse. Because of this, if a negative-dispersion temporal compressor, capable of compressing positively frequency-chirped pulses, is used, the negatively chirped part of the pulse remains uncompressed. As a result, the pulse has a low-intensity pedestal (Fig. 1, A3), which considerably reduces the pulse contrast. In the case of a  $\text{sech}^2$  input laser pulse, after compression its pedestal of  $\sim 200$  fs duration accounts for 38% of the

pulse energy. Note also that, in a ‘dispersionless’ case, the relative pedestal energy is only determined by the initial laser pulse shape. For example, in the case of a Gaussian pulse, the relative pedestal energy under the same conditions is 39%.

Taking into account the dispersion in the silica fibre leads to qualitative changes in calculation results (Fig. 1, columns B, C). It is known [16] that the combined effect of nonlinear self-phase modulation and dispersion-induced pulse broadening processes allows for pulse steepening and makes it possible to obtain a chirp of the same sign essentially throughout the laser pulse. As seen in Fig. 1, in the case of a 2-cm-long fibre (column B) the chirp changes sign only in the low-intensity pulse wings (Fig. 1, B1), which allows the contrast of the compressed pulse to be improved. The relative pedestal energy is here 11%. This is accompanied by an increase in pulse duration and a change in pulse shape at the fibre output. The light intensity falls off during pulse propagation through the fibre in comparison with the ‘dispersionless’ case, so we had to increase the fibre length in our calculations from 0.9 (zero dispersion) to 2 cm in order to maintain the pulse spectral bandwidth.

Further increasing the fibre length does not extend the spectral range of a linear chirp. The spectral range corresponding to a linear chirp is  $\sim 400$  THz in width at both 2-

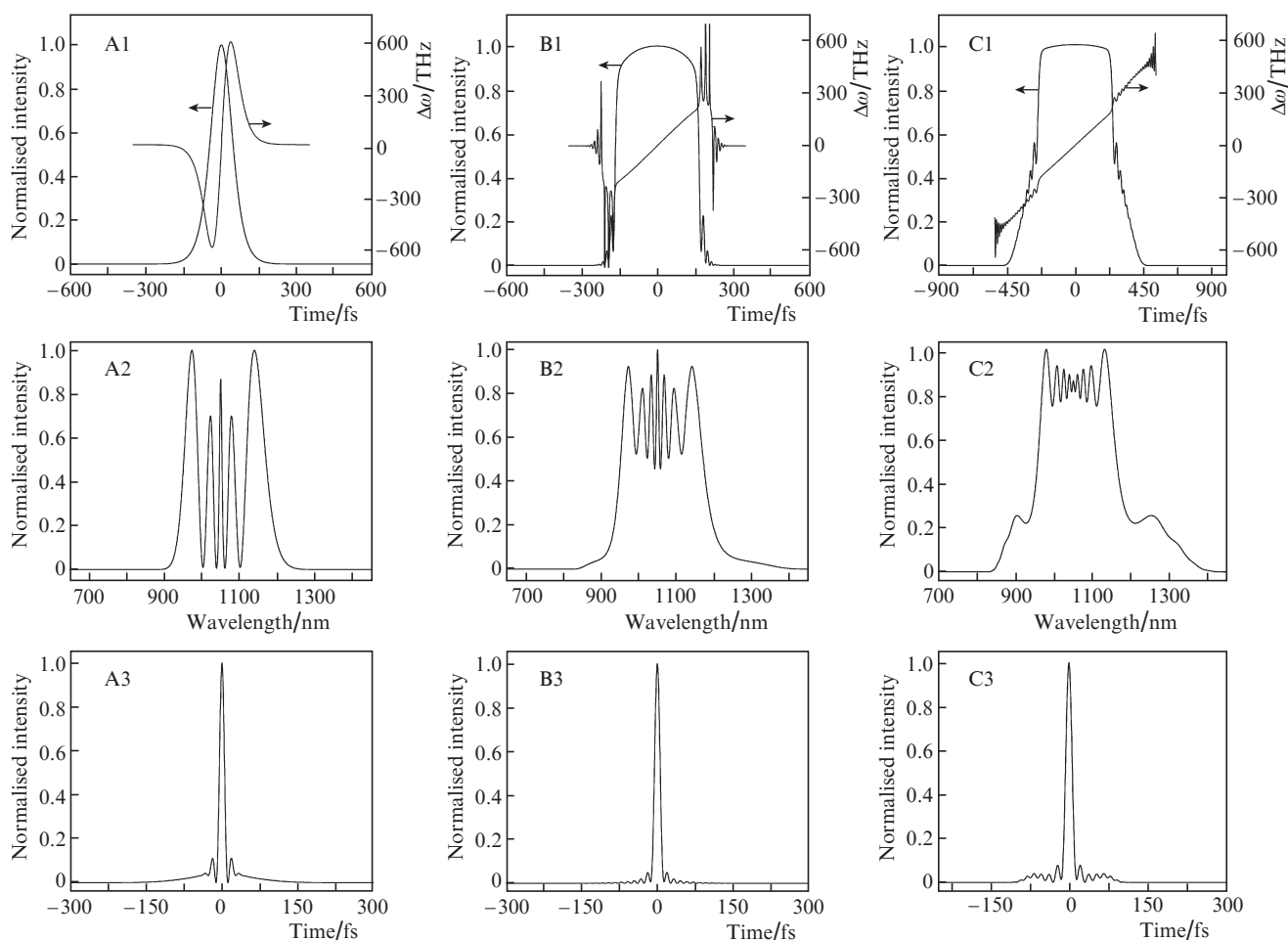


**Figure 1.** Calculated pulse parameters at the fibre output. Column A: fibre length, 0.9 cm (with no allowance for the dispersion in silica glass); column B: fibre length, 2 cm; column C: fibre length, 4 cm; row 1: pulse shape at the fibre output and time variation of the instantaneous frequency detuning  $\Delta\omega$  ( $\Delta\omega = \omega - \omega_0$ , where  $\omega$  is the instantaneous frequency and  $\omega_0$  is the centre frequency of the pulse); row 2: spectra of the pulse; row 3: pulse shape after temporal compression.

and 4-cm fibre lengths (Fig. 1, B1, C1). Note that the total spectral bandwidth rises with increasing fibre length owing to the broadening of the nonlinearly chirped part of the spectrum. A similar picture is observed in the time domain. The extent of the region where the frequency varies linearly is independent of fibre length, and a linear chirp emerges only in the central (most intense) part of the pulse with steep edges (Fig. 1, pulses B1, C1). Therefore, the magnitude of the nonlinear chirp is independent of fibre length, and an optical component with a constant negative dispersion can be used for subsequent temporal pulse compression at the output of fibres differing in length.

In addition, our calculations demonstrate that, at a fibre length less than 2 cm, the spectrum narrows down and, accordingly, the pulse duration after compression increases, without considerable changes in the relative energy of the main peak.

The formation of a nonlinear chirp can be accounted for in terms of the dynamics of changes in the amplitude of the wave and spectrum at the pulse edges (optical wave breaking) [13, 17]. The essence of this effect is that, in a normal dispersion medium, as a consequence of the combined effect of self-phase modulation and dispersion-induced time delay, waves differing in frequency appear at the same point of space. This leads to the generation of new spectral components as a result of nonlinear four-wave processes and, as a consequence, characteristic additional peaks emerge in the spectrum of the pulse [13, 17]. In the spectrum calculated by us, such peaks are located around wavelengths of 900 and 1250 nm (Fig. 1, C2). The fact that a nonlinear chirp cannot be fully compensated by optical components with a second-order nonlinear dispersion degrades the quality of the pulse. The present calculation results demonstrate that, at a compressed pulse duration of  $\sim 12$  fs, which is determined by the width of the linearly chirped part of the spectrum, increasing the fibre length from 2 to 4 cm leads to an increase in the relative energy of the low-intensity pedestal from 11% to 24%.

The limited pulse spectral bandwidth in the self-phase modulation process in silica fibre in the normal dispersion region can be accounted for by the decrease in intensity due to the temporal pulse broadening during propagation in a nonlinear medium. To obtain a wider limiting spectrum, it is necessary to raise the light intensity in the fibre, which makes it possible to reduce the fibre length and the effect of dispersion. The maximum possible intensity is determined by the optical breakdown threshold of the medium, which in turn depends on the pulse duration and laser wavelength.

The above leads us to conclude that, in the case of self-phase modulation in fibre in the normal dispersion region at given laser pulse parameters, there are a limiting bandwidth of a spectrum with a linear chirp and, accordingly, a limiting degree of compression (the minimum pulse duration after a compressor with a negative second-order dispersion). Note that, to obtain high-contrast pulses, it is necessary to optimise the fibre length.

### 3. Experimental results

We experimentally studied the compression of pulses of a TEMA femtosecond ytterbium fibre laser (Avesta Project). The average laser power was up to 5 W, with a pulse repetition rate of 70 MHz. The pulse duration was 100 fs and the centre wavelength was 1050 nm.

The experimental configuration is schematised in Fig. 2. The laser beam was focused onto the input end of an HI 1060 FLEX single-mode silica fibre, with a mode field diameter of 4  $\mu\text{m}$ . Optical isolation between the silica fibre and laser was ensured by a Faraday isolator (Avesta Project). In conjunction with a half-wave plate, it acted as a variable laser power attenuator. The positive dispersion contributed by the optical isolator was compensated for by two chirped mirrors with a total negative dispersion of  $-2000 \text{ fs}^2$ .

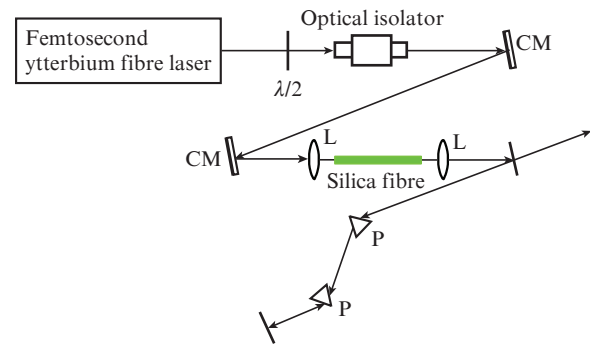


**Figure 2.** Optical layout of the experimental setup: (CM) chirped mirror; (L) lens; (P) prism; ( $\lambda/2$ ) half-wave plate.

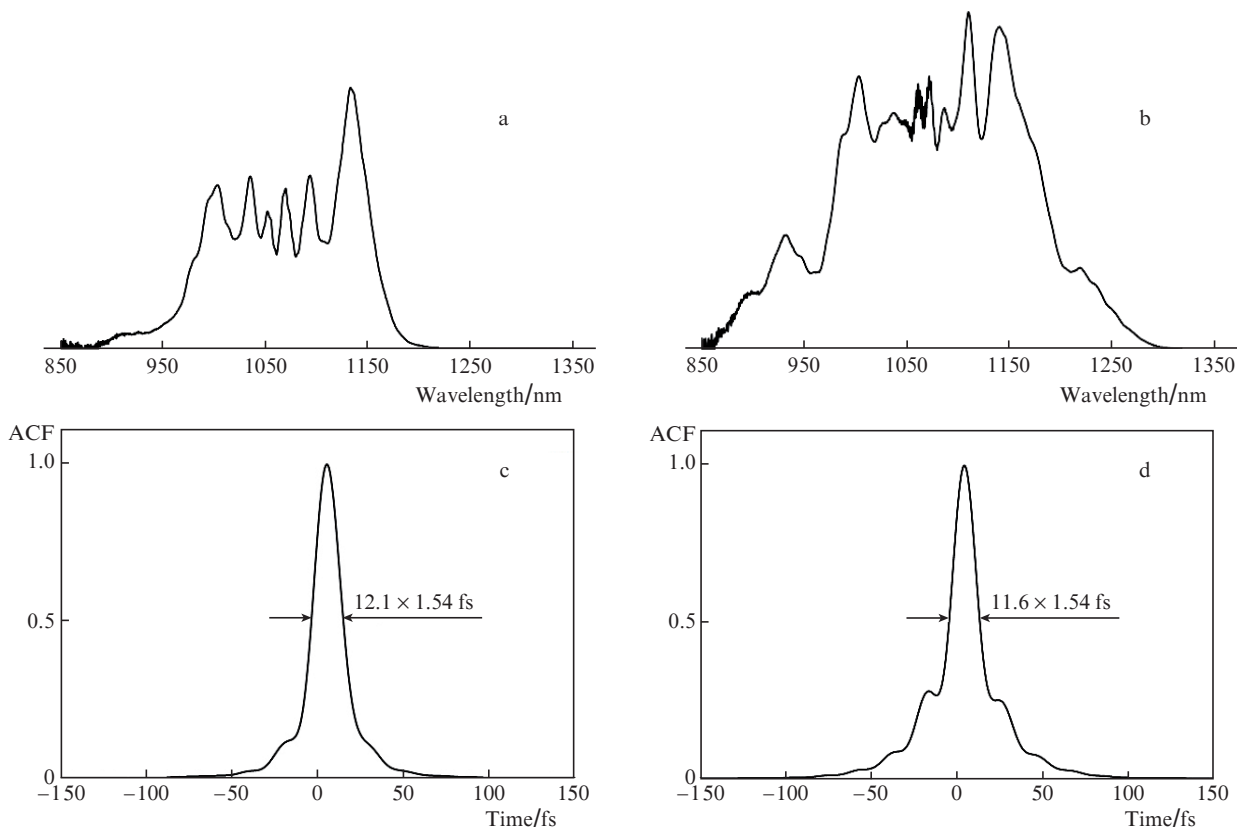
At the fibre output, the light was collimated by a lens and directed to a quartz prism temporal compressor, whose dispersion could be gradually varied by changing the separation between the prisms. The compressed pulse duration was measured by an AA-10DD-12PS scanning autocorrelator (Avesta Project). The output emission spectrum was recorded by an ASR-IR-1.7 scanning spectrometer (Avesta Project).

Figure 3 presents the experimental data obtained for 2- and 4-cm lengths of silica fibre. The average laser power incident on the fibre input end was 1200 mW, which corresponded to a pulse energy of 17 nJ. The average power at the fibre output was 800 mW in both cases, suggesting that the laser light launching loss prevailed. With no significant loss in the prism compressor, the energy efficiency of the entire system was up to 65%.

As seen in Fig. 3, increasing the fibre length leads to spectral broadening and produces extra peaks at the edges of the spectrum, in agreement with the above calculation results. The compressed pulse duration varies insignificantly with fibre length and (under the assumption that the pulse is  $\text{sech}^2$  shaped) is 11.6 fs at a fibre length of 4 cm and 12.1 fs at a fibre length of 2 cm. The relative pedestal energy increases from 12% to 30% as the fibre length is increased to 4 cm. It is also worth noting that, at both fibre lengths, extremely small changes in the separation between the prisms of the compressor were sufficient to maintain a constant compressed pulse duration. This suggests that the linearly chirped parts of the pulses had identical durations and supports the calculation results demonstrating that the magnitude of the linear chirp is independent of fibre length (Fig. 1, B1, C1).

The measured spectra of the pulses (Figs 3a, 3b) are in reasonable agreement with the calculated spectra (Fig. 1, B2, C2). With increasing fibre length, the modulation depth in the spectra decreases and additional peaks emerge.

The present calculation results were used in compressing pulses of a high-power femtosecond ytterbium fibre laser. The



**Figure 3.** (a, b) Measured spectra and (c, d) autocorrelation functions (ACFs) of compressed pulses for (a, c) 2- and (b, d) 4-cm lengths of HI 1060 FLEX fibre.

average laser power incident on the fibre input end was raised to 4.2 W. Accordingly, the pulse energy was 60 nJ. To prevent damage to the silica fibre and maintain the light intensity in the fibre at the level of the preceding experiments, we used 1060-XP fibre, with a mode field diameter of 7  $\mu\text{m}$ . To raise the efficiency, improve the operation stability and reduce the dimensions of the system, a pair of chirped mirrors was used as a temporal compressor. The fibre length was reduced to 1.2 cm in order to match the emission spectrum at the fibre output to the spectral range where the negative dispersion of the chirped mirrors (Layertec,  $-100 \pm 20 \text{ fs}^2$  in the wavelength range 980–1140 nm) was roughly constant. As a result, the

spectrum became slightly narrower and the compressed pulse duration increased in comparison with the 2-cm-long fibre (Fig. 4). After the compression, the pulse duration was 13.2 fs (for a  $\text{sech}^2$  shape). The relative energy of the low-intensity pedestal remained sufficiently low: no higher than 13%. Accordingly, the relative energy of the main pulse, of 13 fs duration, was 87%. With the chirped mirrors, the average power at the compressor output was up to 3.1 W, which corresponds to a 74% energy efficiency of the compressor. The higher compressor efficiency in comparison with that obtained with HI 1060 FLEX fibre is due to the lower laser light launching loss at the larger mode field diameter of the

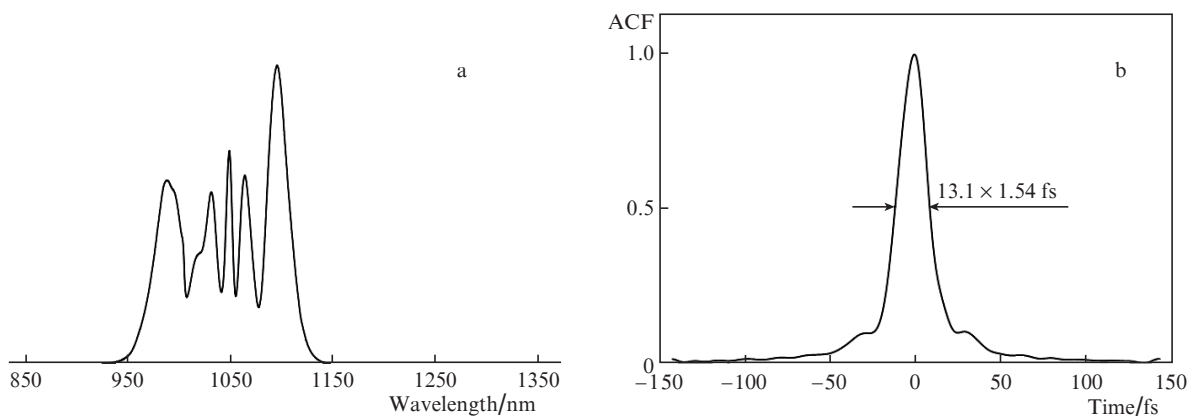


**Figure 4.** (a) Measured spectrum and (b) autocorrelation function of a compressed pulse for a 1.2-cm length of 1060-XP fibre.

fibre. The compression increased the pulse peak power by a factor of 4.9.

#### 4. Conclusions

The following results have been obtained in this study:

1. It has been shown using numerical simulation that, in the case of femtosecond laser pulse compression via nonlinear self-phase modulation in a normal dispersion fibre, followed by chirped pulse propagation through an optical component with a negative second-order dispersion, there is an optimal fibre length which maximises the compressed pulse contrast (i.e. minimises the energy of the low-intensity pulse pedestal) without changing the duration of the main peak.

2. Using a nonlinear fibre compressor, 100-fs ytterbium fibre laser pulses (average output power, 4.2 W; pulse repetition rate, 70 MHz) have been compressed to a 13-fs duration with a 74% efficiency. The associated reduction in the relative energy of the low-intensity pedestal to 13% has made it possible to raise the laser pulse peak power after temporal compression by a factor of 4.9.

#### References

1. Muller M., Kienel M., Klenke A., Gottschall T., Shestaev E., Plotner M., Limpert J., Tunnermann A. *Opt. Lett.*, **41**, 3439 (2016).
2. Schultz M., Prochnow O., Ruehl A., Wandt D., Kracht D., Ramachandran S., Chalmi S. *Opt. Lett.*, **32**, 2372 (2007).
3. Nisoli M., De Silvestri S., Svelto O. *Appl. Phys. Lett.*, **68**, 2793 (1996).
4. Didenko N.V., Konyashchenko A.V., Kostryukov P.V., Losev L.L., Pazyuk V.S., Tenyakov S.Yu., Bryukhanov V.V. *Quantum Electron.*, **46**, 675 (2016) [*Kvantovaya Elektron.*, **46**, 675 (2016)].
5. Russell P.St.J., Holzer P., Chang W., Abdolvand A., Travers J.C. *Nat. Photonics*, **8**, 278 (2014).
6. Druon F., Georges P. *Opt. Express*, **12**, 3383 (2004).
7. Jocher C., Eidam T., Hadrich S., Limpert J., Tunnermann A. *Opt. Lett.*, **37**, 4407 (2012).
8. Buldt J., Muller M., Klas R., Eidam T., Limpert J., Tunnermann A. *Opt. Lett.*, **42**, 3761 (2017).
9. Konyashchenko A.V., Kostryukov P.V., Losev L.L., Tenyakov S.Yu. *Quantum Electron.*, **42**, 231 (2012) [*Kvantovaya Elektron.*, **42**, 231 (2012)].
10. Akhmanov S.A., Vysloukh V.A., Chirkin A.S. *Usp. Fiz. Nauk*, **149**, 450 (1986).
11. Nikolaus B., Grischkowsky D. *Appl. Phys. Lett.*, **42**, 1 (1983).
12. Reilly M.E., McCracken R.A., Farrell C., Reid D.T. *J. Appl. Res. Technol.*, **13**, 555 (2015).
13. Tomlinson W.J., Stolen R.H., Johnson A.M. *Opt. Lett.*, **10**, 457 (1985).
14. Tomlinson W.J., Stolen R.H., Shank C.V. *J. Opt. Soc. Am. B*, **1**, 139 (1984).
15. Konyashchenko A.V., Kostryukov P.V., Losev L.L., Tenyakov S.Yu. *Quantum Electron.*, **41**, 989 (2011) [*Kvantovaya Elektron.*, **41**, 989 (2011)].
16. Grischkowsky D., Balant A.C. *Appl. Phys. Lett.*, **41**, 1 (1982).
17. Anderson D., Desaix M., Lisak M., Quiroga-Teixeiro M.L. *J. Opt. Soc. Am. B*, **9**, 1358 (1992).